

## Surface Modifications Induced by Adsorbates at Low Coverage: A Scanning-Tunneling-Microscopy Study of the Ni/Si(111) $\sqrt{19}$ Surface

R. J. Wilson and S. Chiang

*IBM Almaden Research Center, San Jose, California 95120*

(Received 22 December 1986)

Scanning-tunneling-microscope images of the  $\sqrt{19}$  reconstruction of Ni/Si(111) are shown to rule out existing models for this surface. A new model, based on Si adatom stabilization and sixfold-coordinated Ni sites, is shown to give excellent agreement with the images and to explain the origin of the unit-cell geometry and some surface defects. The results demonstrate that nickel atoms, through Si adatom bonding, have strong effects on the bonding of first-, second-, and third-nearest-neighbor Si surface atoms. This realization provides important insight into the mechanism whereby very small quantities of nickel on the Si(111) surface completely alter the surface structure.

PACS numbers: 68.35.Bs, 68.55.Rt

The ability of small amounts of metallic adsorbates to induce dramatic changes in the structure of semiconductor surfaces has puzzled surface scientists for many years. One example of such a system is the Ni/Si(111) surface. For this system it is known that nickel atoms, at concentrations of a few percent, can induce a complete restructuring of the surface. The determination of the structure of this modified surface has proved extremely difficult because of the large size of the unit cell involved. In this Letter we apply scanning tunneling microscopy (STM) to determine the atomic geometry of the large unit cell of the  $(\sqrt{19} \times \sqrt{19})R23.4^\circ$  Ni/Si(111) reconstruction, hereafter referred to as the  $\sqrt{19}$  structure. Our results demonstrate that all previous models for this surface are incorrect, and that relatively simple considerations of the Ni binding site and a novel form of Si adatom bonding, known to be important for the Si(111)  $7 \times 7$  surface, lead to a model in excellent agreement with images obtained by STM. We find that this model helps to explain surface dislocations and anomalous cells, observed by STM, and provides physical insight into both the origin of this intriguing geometric arrangement and the effectiveness of nickel in altering surface structure.

The  $\sqrt{19}$  reconstruction of the Ni/Si(111) surface has been of interest for many years.<sup>1</sup> Early low-energy electron-diffraction (LEED) studies suggested that this structure was a reconstruction of the clean Si(111) surface. Indeed, the  $7 \times 7$  or  $\sqrt{19}$  structures were obtained on the same sample depending upon the annealing conditions.<sup>2</sup> This observation prompted models based on chains of silicon atoms residing on the surface. Subsequent work revealed that impurities were involved and that annealing parameters controlled the impurity concentration through surface segregation effects.<sup>3</sup> These observations suggested surface compounds which could be epitaxially accommodated only by large unit cells.<sup>4</sup> A model proposing that the  $7 \times 7$  and  $\sqrt{19}$  reconstructions were clean surfaces with patches of displaced atoms around key sites was also considered.<sup>5</sup> More recently, coverage measurements and ultraviolet-photoemission-

spectroscopy (UPS) data have led to models with one Ni atom per unit cell residing within the topmost double layer in a sixfold coordinated site resembling the fluorite structure of NiSi<sub>2</sub>.<sup>6</sup> The surrounding Si atoms were presumed to be displaced from their bulk positions in a manner similar to the distortions proposed at that time for the  $7 \times 7$  reconstruction. A more direct assessment of the Ni site geometry was obtained by surface extended x-ray-absorption fine structure (SEXAFS) which demonstrated high coordination of Ni atoms deposited onto room-temperature Si(111)  $7 \times 7$  substrates.<sup>7</sup> However, the recent determination of the dimer-adatom-stacking-fault (DAS) structure of the Si(111)  $7 \times 7$  surface<sup>8</sup> does not support the displacement model<sup>6</sup> for surface Si atoms. Further interest in  $\sqrt{19}$  structures has been generated by studies of nickel silicide interfaces.<sup>9</sup> It has been shown, for example, that deposition and annealing of small quantities of nickel to produce the  $\sqrt{19}$  structure can strongly influence the subsequent growth<sup>10</sup> of nickel silicide.<sup>11</sup> Finally, we note that a model for a  $\sqrt{19}$  reconstruction on GaAs(111) has recently been proposed<sup>12</sup> on the basis of theoretical calculations on small subunits of the primitive cell.

The measurements described here were carried out on *p*-type Si(111) samples, cleaned by flashing to 1030 °C. This procedure results in surfaces which routinely allow observation of  $7 \times 7$  STM images.<sup>13</sup> High-purity Ni was evaporated from an alumina-coated tungsten basket source at a rate of 0.3 Å/min at pressures below  $4 \times 10^{-10}$  Torr. LEED patterns showing diffuse  $\sqrt{19}$  structure were readily obtained by annealing of samples, coated with Ni at room temperature, at 1000 °C for 1 min followed by radiation quenching to room temperature.<sup>1</sup> Other techniques for the preparation of  $\sqrt{19}$  are also known.<sup>9,10</sup> Auger measurements of the Ni concentration in the first few monolayers showed that Ni was present in amounts corresponding to about 0.2 monolayer. This value is larger than one Ni atom per nineteen top-layer Si atoms, necessary to stabilize the  $\sqrt{19}$  cell,<sup>6</sup> and presumably caused, along with the radiative quench-

ing, the diffuse LEED patterns. Samples were then transferred into the STM<sup>14</sup> and constant-current slow-scan images were recorded at various gap voltages.<sup>15-18</sup>

The most prominent features of the STM images are

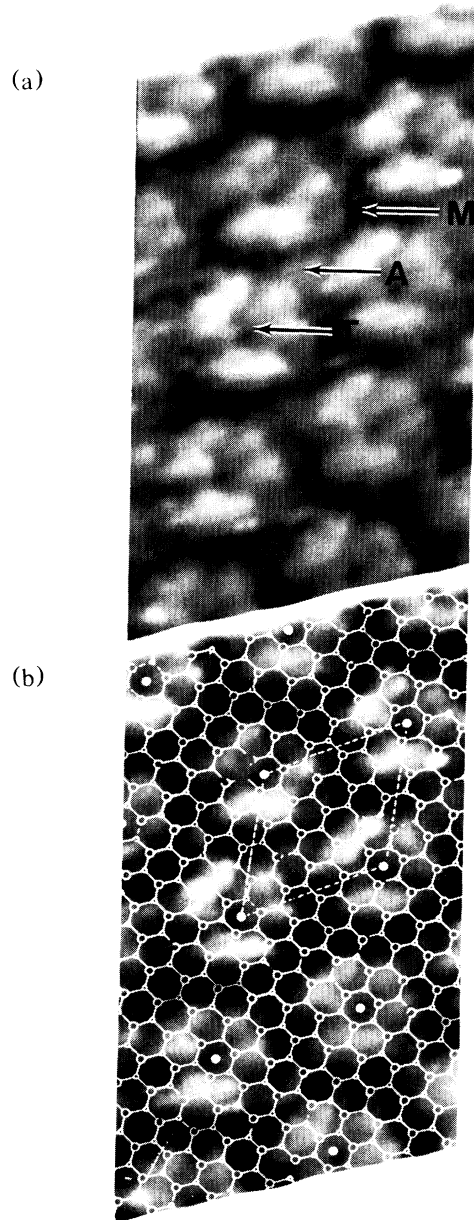


FIG. 1. (a) STM image of the Ni/Si(111)  $\sqrt{19}$  surface over a  $(70 \times 90)\text{-}\text{\AA}^2$  region. The tunneling current is 0.2 nA and the sample-tip bias voltage is  $-1.2$  V for tunneling into filled states of the sample. The  $\sqrt{19}$  cell edges are known to be  $16.65$   $\text{\AA}$  long. All labels are defined in the text. (b) The previous image magnified and overlaid with the unreconstructed surface mesh of Si(111). The positions of the individual balls at the cell corners fall near threefold hollow sites of the unreconstructed surface for this mesh registration. Solid white circles mark the unit cell corners.

the threefold structures ( $T$ ) evident in Fig. 1(a). The spacing of the unit cell formed by these structures was found to be consistent with the  $\sqrt{19}$  structure by comparison with data obtained on the Si(111)  $7 \times 7$  surface. The corrugation associated with the threefold corner structures was found to be about  $3$   $\text{\AA}$  over a range of gap voltages and for either polarity. It is unlikely that the electronic density of states can account for this larger corrugation and surface atoms must be involved. Nickel coverage<sup>6</sup> and coordination number<sup>7</sup> rule out the possibility of surface Ni atoms. In fact the diameter of the six, barely resolved, individual balls in the corner structures strongly resembles those of Si adatoms of the  $7 \times 7$  surface.<sup>15-17</sup> In the present case we find, consulting Fig. 1(b), that the six balls are separated from each other by about  $3.8$   $\text{\AA}$ . This is very different from the DAS model where adatoms are separated by twice this distance. At this larger separation, each adatom can satisfy three top-layer dangling bonds and thereby lower the total energy. This mechanism cannot operate at the closer spacing unless additional broken bonds in the surface are present. Also exceptional are the large corrugation and pronounced pairing, possibly an electronic structure effect, which are evident in all of our images. A consideration of the Ni binding site determined by SEX-AFS<sup>7</sup> offers further insight into these threefold features. Ni atoms were found to reside in the sixfold hollow site between the first and second Si layers. The Ni—Si bond length was determined and requires that the adjacent top-layer Si atoms buckle outwards by about  $0.8$   $\text{\AA}$ . As a result, interlayer Si—Si bonds break and result in the configuration shown in Fig. 2(a). This rearrangement leads to a high bond density on silicon atoms bonded to

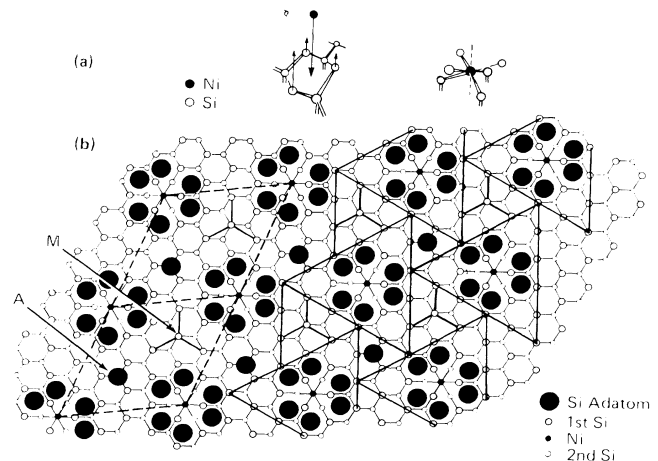


FIG. 2. (a) Two perspective views of the Si(111) surface before and after the introduction of an intralayer Ni atom (Ref. 7). (b) Top view of the Ni site showing surrounding top-double-layer Si atoms and adatom positions inferred from Fig. 1(b). The left portion shows two unit cells and the right side shows a construction using close-packed triangles (Ref. 12).

the Ni atom. In Fig. 2(b) we show the Ni site embedded in the Si(111) surface. If we reconnect the bonds between the Ni site and the surrounding surface, as shown, we find that there are two bonds associated with each top-layer and one with each bottom-layer Si atom in the cluster about the Ni atom. This corresponds to the breaking of one bond between top- and second-layer Si atoms upon insertion of the Ni atom. When these bonds are added to the dangling bonds of the top-layer atoms surrounding the cluster, it becomes possible to have three bonds to each of six adatoms in the sites shown in Fig. 2(b). All broken bonds are then satisfied, except for one dangling bond per adatom, in this region. Some ambiguity remains regarding the precise position and hybridization of both first- and second-layer Si atoms bonded to the Ni atom because the Ni-site geometry is not compatible with tetrahedral Si. In any case, the outward buckling and high bond density of the Si atoms adjacent to the Ni site, together with a typical 2-Å adatom corrugation,<sup>15-17</sup> nicely explain the large observed corrugation, close spacing, and the threefold symmetry of these features.

An examination of the rest of the unit cell shown in Fig. 2(b) shows that seven top-layer atoms remain as yet unassociated with adatoms. Three of these occur as adjacent top-layer sites (*A*) where, by analogy with the DAS model, adatoms would be expected. The four remaining dangling bonds do not form a threefold hollow site and should appear as a Y-shaped minimum (*M*) of the corrugation. These predicted features can be observed in most of the cells in Fig. 1(a) and in the empty-state image shown in Fig. 3(a). Evidently these arguments explain all features of the unit cell and form the basis for our choosing the mesh registration shown in Fig. 1(b). The fact that atoms beneath the adatom layer are not resolved is expected from other work on Si(111) 7×7 surfaces.<sup>15-17</sup> Faulting within the unit cell appears unlikely because of the misorientation of the unit cell with respect to the Si lattice. We do, however, expect significant local distortions of the Si lattice near the Ni site.

For tunneling into empty states we observe similar well-ordered Ni site structures as exemplified by Fig. 3. The resolution which we have obtained in this polarity is somewhat less than for filled-state images. This is reasonable since states above the Fermi level are more delocalized and extend further into the vacuum than do their occupied counterparts. As a further check on our model we test whether it can account for defects found in some regions of Fig. 3(a). Consulting an overlay, shown in Fig. 3(b), we find that all Ni sites are centered over sixfold hollow sites. This is true even near the surface dislocation (*D*) which was observed in four consecutive images. When the Ni sites are more closely spaced than normal an adatom is eliminated (*E*). In portions of the image where the corner sites are excessively separated,

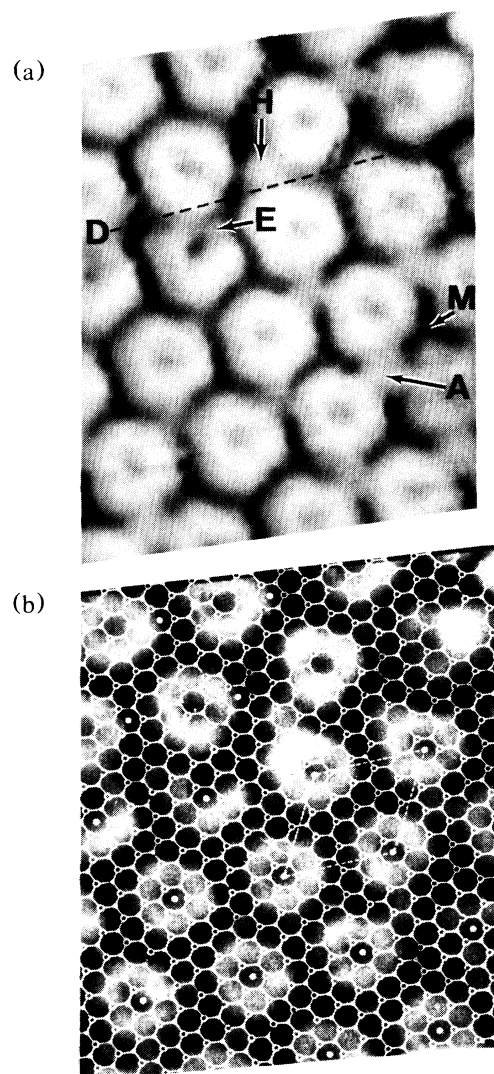


FIG. 3. (a) An STM image, recorded at 0.2 nA and +1.90 V, showing both ordered and defective regions. Symbols are defined in the text. (b) Same image with Si(111) surface mesh superimposed to show registration of Ni sites.

an additional adatom appears when a threefold hollow site (*H*) is available. By the use of such ideas essentially every feature observed in these images can be understood. In Fig. 4 we show an image taken over a larger area. Now both domains (*R1* and *R2*) can be seen along with a dislocation (*D*) and a disordered area (*A*). This disordered area is evidently comprised only of the threefold structures associated with Ni atoms together with isolated adatoms filling in the empty spaces. We regard the persistence of the threefold structures into disordered regions as strong evidence for considering them to be independent stable subunits associated with Ni atoms in sixfold hollow intralayer sites.

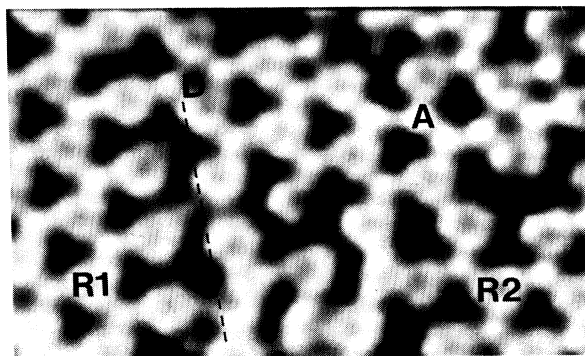


FIG. 4. Image of a larger region, recorded at 0.2 nA and +1.20 V, which shows a variety of different structures defined in the text. The scanned area is too large to allow registration relative to the surface mesh.

The origin of the unusual  $\sqrt{19}$  geometry can be approached by consideration of the influence of the defects shown in Fig. 3. Evidently any attempt to pack the Ni sites more closely, as is the case near the dislocation (*D*) in Fig. 3, results in destabilization of the reconstruction by elimination of an adatom (*E*). Larger cells appear to be prohibited by attempts of the system to close pack the threefold Ni+Si adatom units. In fact, it has been shown that the closest packing of the Ni+Si adatom sites, included within the large equilateral triangles in Fig. 1(b), actually requires a  $\sqrt{19}$  structure.<sup>12</sup> These considerations demonstrate that, by virtue of Si adatoms, the effects of one Ni atom result in large alterations in the bonding of at least eighteen Si atoms. Thus the strong effects of Ni at low coverage can be readily understood.

Our results can be summarized as follows. We have used STM to obtain images of the  $\sqrt{19}$  Ni/Si(111) surface at various gap voltages. Threefold structures with 3-Å corrugation correspond precisely to the images which would be expected for Si adatom binding to Si dangling bonds on sites adjacent to embedded Ni atoms. A consideration of the remaining dangling bonds in the unit cell shows that those which are arranged around a threefold hollow site are also bonded to adatoms while those in a less compact geometry are not. The observation of disordered regions composed of identical three-

fold structures mixed with isolated adatoms shows the threefold structures to be subunits which are stable independent of the surroundings. Adatom stabilization provides a mechanism whereby Ni atoms alter the chemical bonding of many surrounding Si atoms thereby explaining the large effects at low coverage. Finally, an examination of defect structures shows that the  $\sqrt{19}$  structure represents the most close-packed arrangement of these Ni+Si adatom units which is stable and explains the origin of this unusual geometry.

The authors are pleased to acknowledge useful discussions with I. P. Batra and H. Morawitz and the assistance of Ch. Cerber in the construction of the instrument.

- 
- <sup>1</sup>R. E. Schlier and H. E. Farnsworth, *J. Chem. Phys.* **30**, 917 (1959).  
<sup>2</sup>R. Seiwatz, *Surf. Sci.* **2**, 473 (1964).  
<sup>3</sup>A. J. Van Bommel and F. Meyer, *Surf. Sci.* **8**, 467 (1967).  
<sup>4</sup>E. Bauer, in *Proceedings of the Fourth International Materials Symposium, The Structure and Chemistry of Solid Surfaces*, edited by G. A. Somorjai (Wiley, New York, 1969), Paper No. 23.  
<sup>5</sup>G. Le Lay, *Surf. Sci.* **108**, L429 (1981).  
<sup>6</sup>G. V. Hansson, R. Z. Bachrach, R. S. Bauer, and P. Chiaradia, *Phys. Rev. Lett.* **46**, 1033 (1981).  
<sup>7</sup>F. Comin, J. E. Rowe, and P. H. Citrin, *Phys. Rev. Lett.* **51**, 2402 (1983).  
<sup>8</sup>K. Takayanagi, Y. Tanashiro, S. Takahashi, and M. Takahashi, *Surf. Sci.* **164**, 367 (1985).  
<sup>9</sup>J. G. Clabes, *Surf. Sci.* **145**, 87 (1984).  
<sup>10</sup>G. Akinci, T. Ohno, and E. D. Williams, to be published.  
<sup>11</sup>R. T. Tung, J. M. Gibson, and J. M. Poate, *Phys. Rev. Lett.* **50**, 429 (1983).  
<sup>12</sup>E. Kaxiras, Y. Bar-Yam, J. D. Joannopoulos, and K. C. Pandey, *Phys. Rev. Lett.* **57**, 106 (1986).  
<sup>13</sup>R. J. Wilson and S. Chiang, *Phys. Rev. Lett.* **58**, 369 (1987).  
<sup>14</sup>S. Chiang and R. J. Wilson, *IBM J. Res. Dev.* **30**, 515 (1986).  
<sup>15</sup>G. Binnig, H. Rohrer, C. H. Gerber, and E. Weibel, *Phys. Rev. Lett.* **50**, 120 (1983).  
<sup>16</sup>J. A. Golovchenko, *Science* **232**, 48 (1986).  
<sup>17</sup>R. J. Hamers, R. M. Tromp, and J. E. Demuth, *Phys. Rev. Lett.* **56**, 1164 (1986).  
<sup>18</sup>J. A. Stroscio, R. Feenstra, and A. P. Fein, *Phys. Rev. Lett.* **57**, 2579 (1986).

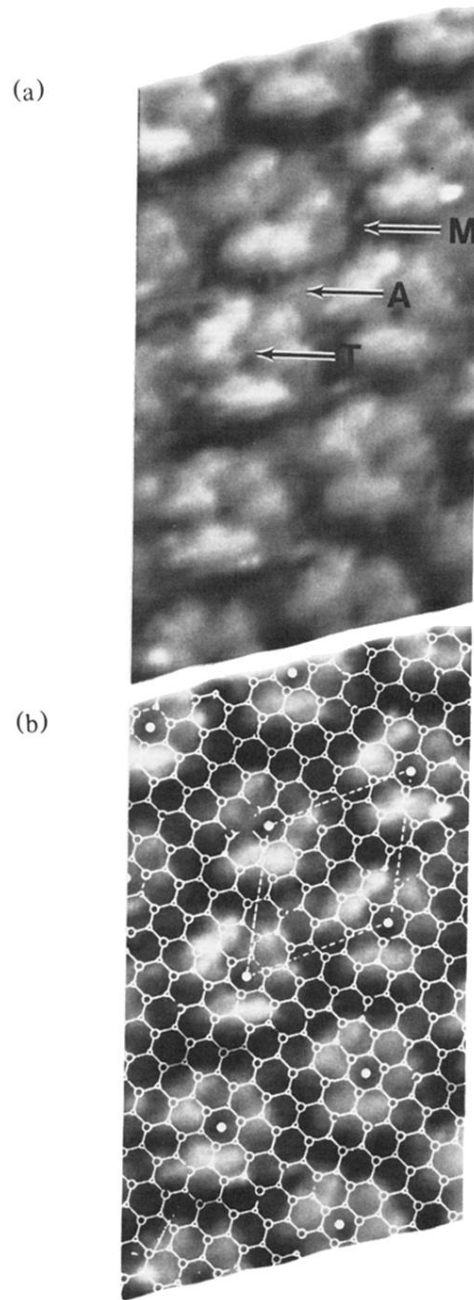


FIG. 1. (a) STM image of the Ni/Si(111)  $\sqrt{19}$  surface over a  $(70 \times 90)\text{-}\text{\AA}^2$  region. The tunneling current is 0.2 nA and the sample-tip bias voltage is  $-1.2$  V for tunneling into filled states of the sample. The  $\sqrt{19}$  cell edges are known to be  $16.65$   $\text{\AA}$  long. All labels are defined in the text. (b) The previous image magnified and overlaid with the unreconstructed surface mesh of Si(111). The positions of the individual balls at the cell corners fall near threefold hollow sites of the unreconstructed surface for this mesh registration. Solid white circles mark the unit cell corners.

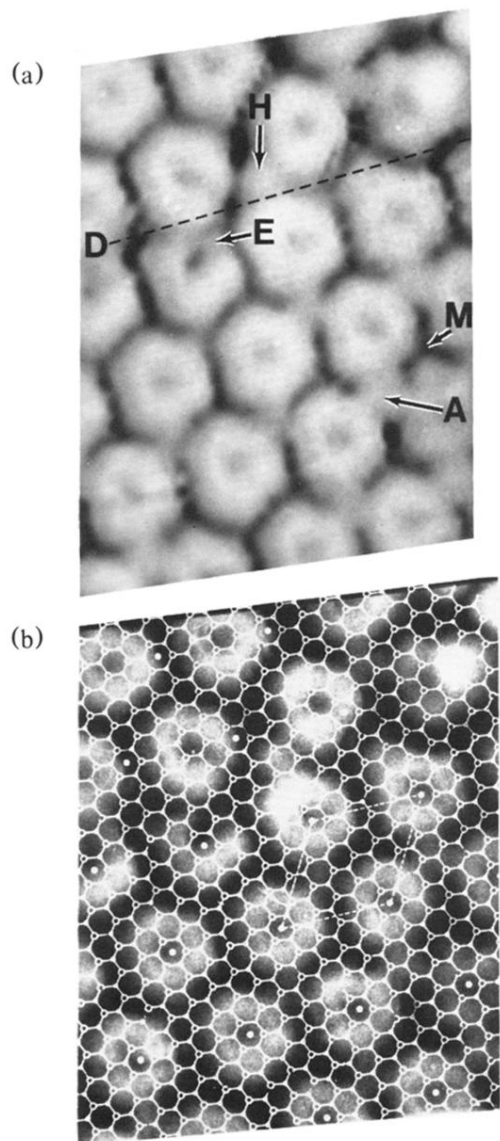


FIG. 3. (a) An STM image, recorded at 0.2 nA and +1.90 V, showing both ordered and defective regions. Symbols are defined in the text. (b) Same image with Si(111) surface mesh superimposed to show registration of Ni sites.

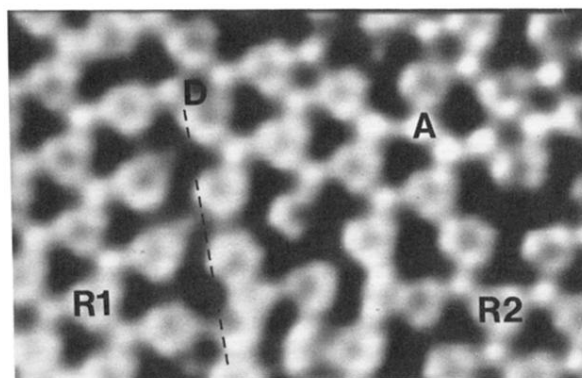


FIG. 4. Image of a larger region, recorded at 0.2 nA and +1.20 V, which shows a variety of different structures defined in the text. The scanned area is too large to allow registration relative to the surface mesh.